

## Experimental Investigations of Magnetic Abrasive Finishing on Titanium

Shadab Ahmad<sup>1\*</sup>, Ranganath M Singari<sup>2</sup>, R S Mishra<sup>3</sup>

(<sup>1,2,3</sup>Delhi Technological University, Delhi 110042)

Email: [shadab.gkp09@gmail.com](mailto:shadab.gkp09@gmail.com)

<https://doi.org/10.35121/ijapie201904236>

**Abstract :** Magnetic abrasive finishing (MAF) is one of the finishing processes which produces nano finished surfaces. The material removal process is in the form of microchips. The present paper introduces a novel work based on the principle of MAF for flat surfaces. The experiments were conducted on titanium material to investigate the response of MAF on hardness. Matlab has been used to evaluate the performance. The results obtained from the experimental investigations revealed that the hardness improves with MAF. The surface morphology of finished surface was studied with the help of SEM images

**Keywords:** Magnetic Abrasive Finishing (MAF), Titanium, Nano finishing, Flat surfaces, Microchips.

### 1. INTRODUCTION

Scientists and engineers are looking for a material which is based on renewable and sustainable resources, environment-friendly, economical and of low cost, high strength and light in weight, ease of recycling etc. The lignocellulosic fiber based material is the best solution due to its varieties of attractive properties over synthetic materials. In recent years, natural fiber-reinforced composites have received attention by automotive and construction industries for making structural parts and building materials. Despite a number of advantageous properties, natural fibers like sisal, banana, coconut coir, sugarcane bagasse, pineapple leaf fiber etc have some limitations like hydrophilic nature, poor wettability with synthetic polymer, low thermal stability, and poor interfacial bonding strength with resin. Most of the researchers have already worked for effective solutions to these problems and find out that physical and chemical treatment of natural fiber surface leads to better compatibility with the polymeric resin. But very few works have been done towards the area of surface treatment effect on thermal stability of natural fibers. Na Lu *et al.* (2013) investigated the effect of surface treatment of hemp fibers on the thermal stability of Hemp-PLA biocomposite. They concluded that the thermal degradation temperature was increased from 330 °C to 340 °C after the treatment of hemp fiber with 5 wt% NaOH solution [1]. Arifuzzaman Khan G M *et al.* (2012) studied the effect of sodium hydroxide on the thermal behavior of coconut husk (coir) fiber. They found that the main degradation temperature peak is shifted to a higher temperature region of about 19 °C [2]. As natural lignocellulosic fibers, they can be subjected to thermo-

chemical decomposition during industrial processing and biocomposite production. It is of practical significance to study for understanding, predicting, and evaluating the thermal decomposition mechanism of lignocellulosic fibers. The knowledge of the thermal decomposition process would help to better design final product by estimating the influence on product properties.

Thermogravimetric analysis (TGA) is one of the most popular and widely used technique to analyze the decomposition process of solid material, kinetic analysis of de-volatilisation process, and it provides possibilities to study the effects of heating rate, temperature, pressure, atmosphere gas, gas flow rate, biomass composition, and particles size on mass loss of a sample. Kinetic analysis of thermo-chemical reactions for the solid mass sample can be done either by a model fitting method or model-free method. Model fitting methods of kinetic analysis require fitting of different models to the kinetic data for obtaining the best statistical fit. The disadvantage of this strategy is the possibility of wrong model selection which results in an error in kinetic parameters. The model-free methods consist of several kinetic curves with the multi-heating rate for estimating the activation energy ( $E_a$ ). Kissinger, Flynn-Wall-Ozawa (FWO), and Friedman are the common and effective methods based on multiple heating rates, increasingly adopted by researchers to analyze the thermo-chemical conversion of natural fiber, kinetic analysis of de-volatilization, and estimation of activation energy. All these model-free methods are summarized in Table 1 [3-5]. Alwani M. Sitiet *al.* (2014) examined the kinetic analysis of SCB, COIR, PALF, and BPS fibers by Kissinger, Friedman, and F.W.O methods.

They concluded that COIR was the most thermally stable fiber followed by PALF, BPS, and SCB. The activation energy of COIR, PALF, SCB, and BPS fibers were 100.84, 96.28, 92.87, and 80.79 (kJ/mol) respectively when calculated by Friedman's method [6]. Yao Fei et al. (2007) studied the thermal decomposition kinetics of 10 types of fibers by Kissinger. They found the activation energy of Bagasse, Bamboo, Cotton Silk, Hemp, Jute, Kenaf, Rice husk, Rice straw, Wood maple, and Wood pine were 161.1, 161.6, 146, 171.1, 165.6, 157.7, 167.4, 176.2, 153.7, 159.3 respectively [7].

Table 1: Kinetic methods used for calculating the activation energy

Methods	Equation	Reference
Kissinger	$\ln \frac{\beta}{T^2} = \ln \frac{AR}{E} - \frac{E}{RT}$	Kissinger, 1957 [2]
Friedman	$\ln \frac{d\alpha}{dt} = \ln[Af(\alpha)] - \frac{E}{RT}$	Friedman, 1964 [3]
F.W.O	$\ln \beta = \log \frac{AE}{Rg(x)} - 5.331 - 1.052 \frac{E}{RT}$	Flynn and Wall, 1966 [4]

The decomposition of natural fibers occurs in two to three stages depends on the type of fiber and its chemical composition. Alwani M. Sitiet *et al.* (2014) reported that SCB and COIR fiber was decomposed in two steps but BPS fiber decomposes in three steps. It was due to the presence of high amount of lignin and cellulose in BPS fiber compared to SCB and COIR [6]. Na Lu *et al.* (2013) concluded that hemp fiber was decomposed in two steps, starting with the loss of moisture around 100 °C and followed by successive decomposition of hemicellulose, cellulose, and lignin in the range of 150-400 °C [1]. According to JayamaniElammaran*et al.* (2014), thermal decomposition of both untreated and treated betel nut fiber polyester composites had two mass loss steps, where 10 wt% mass losses shifted from 110 °C to (120-140) °C after 5 wt% of alkaline treatment [8]. The purpose of this work was to study and analyze the effect of alkaline treatment with different concentrated solutions (2%, 4%, 6%, 8%, and 10 wt %) on thermal stability of pineapple leaf fiber (PALF). The pyrolysis process was performed by TGA machine under the condition of constant heating rate and constant mass flow rate of the gas.

## 2. EXPERIMENTAL

### A. Materials

Raw pineapple leaf fiber (R-PALF) was purchased from Go Green Products, Chennai, India. The average density and moisture content in PALF was equal to 0.98 g/cm<sup>3</sup> and 10-11% respectively. Table 2 shows the chemical composition of the materials [9]. Sodium hydroxide (NaOH) used for alkaline treatment was of laboratory reagent (LR) grade and obtained from the local supplier.

Table 2: Chemical composition of pineapple leaf fiber

Fiber	Cellulose %	Hemicellulose %	Lignin %	Pectin %
PALF	70-82	18.8	5-12.7	1.1

### B. Fiber Treatment

Pineapple leaf fibers were treated by immersing in (2%, 4%, 6%, 8%, and 10 wt %) of alkaline (NaOH) solutions for 24 hrs at 25 °C, followed by washing with deionized water (until the pH was reached 7), and drying in oven at 60 °C for 24 hrs (until the constant weight was maintained). The untreated raw pineapple leaf fibers (R-PALF) were also washed in deionized water and dried at 60 °C for 24 hrs.

### C. Method

1) *Fourier-Transform Infrared Spectroscopy (FTIR)*: Fourier-transform infrared spectroscopy, model Perkin Elmer 2000 was used to analyze the effect of alkali treatment of different concentrations (2%, 4%, 6%, 8% and 10 wt %) on chemical bonding exist in untreated pineapple leaf fiber. FTIR spectra were analyzed with an infrared spectrophotometer in the range 4000 cm<sup>-1</sup> to 400 cm<sup>-1</sup>. FTIR of untreated and alkali treated pineapple leaf fiber had done in CSIR-CSIO analytical instrumentation laboratory.

2) *Thermogravimetric Analysis (TGA)*: Thermogravimetric analysis (TGA) of Pineapple leaf fiber (both untreated and treated) was carried out using a thermogravimetric analyzer (Perkin Elmer, TGA 4000). The samples of mass 5 mg were evenly and uniformly distributed in the alumina crucible which was supported by a precision balance. This small amount of natural fiber was taken for uniformity of temperature throughout the sample. The variation in mass of sample with respect to temperature and time was controlled, monitored and recorded using Perkin Elmer thermal software (Pyris). The temperature change of PALF was controlled from 25 °C to 700 °C at a heating rate of 10°C/min under the high purity nitrogen (inert) atmosphere at a flow rate of 20 ml/min. The heating rate of 10°C/min was selected for better resolution of transition. TGA of COIR and PALF fibers had done in Central Instrumentation Laboratory, DTU (Delhi).

## 4. RESULT AND DISCUSSION

### *Fourier-Transform Infrared Spectroscopy (FTIR)*

Fig. 1 shows the IR spectra for untreated and alkali treated pineapple leaf fiber (PALF) that was obtained by using the FTIR spectrometer.

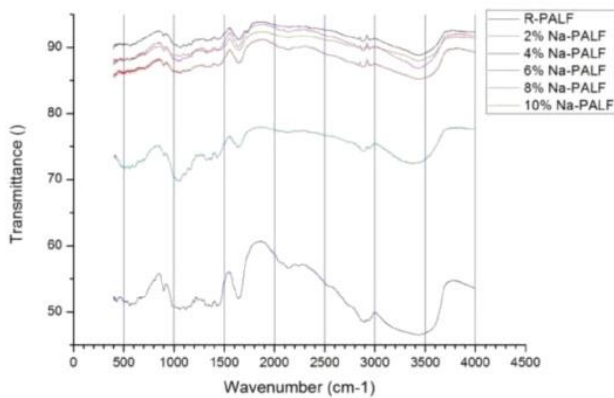


Fig. 1: IR spectra of untreated and alkali treated pineapple leaf fibers

The broad peak between  $3200\text{ cm}^{-1}$  to  $3500\text{ cm}^{-1}$  is linked to OH stretching vibration present in amorphous and crystalline cellulose. The carbonyl stretching ( $\text{C}=\text{O}$ ) peak ( $1730\text{ cm}^{-1}$ ) related to hemicellulose can be seen in untreated PALF but not present in alkali treated pineapple leaf fibers. This may be due to the removal of hemicellulose component.  $\text{CH}_2$  bending peaks at  $1432\text{ cm}^{-1}$  are present in both untreated and alkali treated fiber. The increase in peak intensity at around ( $1600\text{--}1650\text{ cm}^{-1}$ ) after alkaline treatment corresponds to the removal of wax, adhesives, pectin, and gummy substance from the fiber surface. The small peak at  $1525\text{ cm}^{-1}$  is related to lignin component. This peak is not present in the alkali treated sample. It could be due to partial removal of lignin after alkali treatment. The peak at  $1244\text{ cm}^{-1}$  is much smaller in alkali treated PALF than untreated sample. This peak corresponds to  $\text{C}=\text{O}$  stretch of the acetyl group of lignin and is reduced because lignin is partially removed from the fiber surface.

#### Thermal Decomposition of Untreated and Treated Pineapple Leaf Fiber

degrade earlier than treated fiber [1]. Fig. 2 showed that the major mass loss (30-50%) occur at the temperature greater than  $300\text{ }^\circ\text{C}$ . This was because of the decomposition of cellulose and lignin. It was investigated that crystalline cellulose was degraded between the temperatures of  $302\text{--}375\text{ }^\circ\text{C}$ . The DTG curves show that at peak temperature, the rate of decomposition was increased from  $6.83\text{ } \%/ \text{min}$  to  $7.13\text{ } \%/ \text{min}$  due to 4% alkali treatment of pineapple leaf fiber. These results are because of depolymerization of native cellulose structure to short length crystallites. Lignin was the most difficult component to decompose compared to other components because of its cross-linked highly complex aromatic structure of phenylpropane units. It starts to decompose at a lower temperature (typically  $160\text{--}175\text{ }^\circ\text{C}$ ) compared to cellulose but it decomposed slowly under the whole temperature range and extend its temperature as high as  $900\text{ }^\circ\text{C}$ . The DTG curves for untreated and treated pineapple leaf fibers have reached the equilibrium stage beyond  $400\text{ }^\circ\text{C}$  where the rate of decomposition is approximately constant and lignin component of natural fiber decomposes slowly.

According to Paiva et al. (2006), the decomposition of lignin occurred in a wider temperature compared to cellulose and hemicellulose [15]. After  $700\text{ }^\circ\text{C}$ , the remaining mass of pineapple leaf fiber was shown in Table 3. It was observed that the residue was increased up to 8% alkali treated fiber compared to the untreated one. This was due to the slow rate of the chemical decomposition reaction. Only ash and char was left after  $700\text{ }^\circ\text{C}$ . The differences in the amount of char left can be attributed to the change in chemical composition of pineapple leaf fiber after alkali treatment. It was reported by Williams (2004) that a high lignin content in natural fiber results in the production of a higher level of ash and char during pyrolysis [16]. The 10% NaOH treated PALF shows less residue content than untreated PALF. This might be due to excess delignification of pineapple fiber after 10% alkaline treatment.

## 5. CONCLUSIONS

This study concludes that pineapple leaf fibers (both untreated and treated) decompose in two steps due to hemicellulose, cellulose, and lignin decomposition. The major mass loss (30 to 50%) of pineapple leaf fibers were in the range of  $340\text{--}365\text{ }^\circ\text{C}$ . It was attributed due to major decomposition of cellulose.

The initial decomposition temperature of pineapple leaf fiber was increased from  $250\text{ }^\circ\text{C}$  to  $300\text{ }^\circ\text{C}$  after 4 wt% alkaline treatment. It was due to the removal of hemicellulose which results the remaining cellulose occupies a crystalline structure that leads to better thermal stability.

The results depict that 4 wt% alkaline treated pineapple leaf fiber shows maximum thermal stability. The residue content of PALF was increased from 10.89% to 17.24 wt% after 4% alkaline treatment. This elevation was attributable to the change in chemical composition of pineapple leaf fiber.

The maximum rate of decomposition was increased from  $6.85\text{ } \%/ \text{min}$  to  $7.51\text{ } \%/ \text{min}$  after 10 wt% NaOH treatment. This was because of depolymerization of native cellulose to short length crystallites.

#### ACKNOWLEDGMENT

Authors offer the most sincere gratitude to the Council of Scientific and Industrial Research (CSIR), Government of India, for financial support in the form of Junior Research Fellowships.

#### References

#### REFERENCES

- [1] S. Khalaj Amineh, A. Fadaei Tehrani, and A. Mohammadi, "Improving the surface quality in wire electrical discharge machined specimens by removing the recast layer using magnetic abrasive finishing method," *Int. J. Adv. Manuf. Technol.*, Aug. 2012, doi: 10.1007/s00170-012-4459-7.
- [2] J. Guo, J. Bai, K. Liu, and J. Wei, "Surface quality improvement of selective laser sintered polyamide 12 by precision grinding and magnetic field-assisted finishing," *Mater. Des.*, vol. 138, pp. 39–45, Jan. 2018, doi: 10.1016/j.matdes.2017.10.048.
- [3] A. K. Singh, S. Jha, and P. M. Pandey, "Parametric analysis of an improved ball end magnetorheological finishing process," *Proc. Inst. Mech. Eng. Part B J. Eng. Manuf.*, vol. 226, no. 9, pp. 1550–1563, Sep. 2012, doi: 10.1177/0954405412453805.
- [4] D. K. Singh, V. K. Jain, and V. Raghuram, "Parametric study of magnetic abrasive finishing process," *J. Mater. Process.*

- Technol., vol. 149, no. 1–3, pp. 22–29, Jun. 2004, doi: 10.1016/j.jmatprotec.2003.10.030.
- [5] M. Mosavat and A. Rahimi, “Numerical-experimental study on polishing of silicon wafer using magnetic abrasive finishing process,” *Wear*, vol. 424–425, pp. 143–150, Apr. 2019, doi: 10.1016/j.wear.2019.02.007.
- [6] H. Yamaguchi, A. K. Srivastava, M. A. Tan, R. E. Riveros, and F. Hashimoto, “Magnetic abrasive finishing of cutting tools for machining of titanium alloys,” *CIRP Ann.*, vol. 61, no. 1, pp. 311–314, 2012, doi: 10.1016/j.cirp.2012.03.066.
- [7] V. K. Jain, “Magnetic field assisted abrasive based micro-/nano-finishing,” *J. Mater. Process. Technol.*, vol. 209, no. 20, pp. 6022–6038, Nov. 2009, doi: 10.1016/j.jmatprotec.2009.08.015.
- [8] V. K. Jain, “ABRASIVE-BASED NANO-FINISHING TECHNIQUES: AN OVERVIEW,” *Mach. Sci. Technol.*, vol. 12, no. 3, pp. 257–294, Sep. 2008, doi: 10.1080/10910340802278133.
- [9] N. Sihag, P. Kala, and P. M. Pandey, “Chemo Assisted Magnetic Abrasive Finishing: Experimental Investigations,” *Procedia CIRP*, vol. 26, pp. 539–543, 2015, doi: 10.1016/j.procir.2014.07.067.
- [10] S. R. Bhagavatula and R. Komanduri, “On chemomechanical polishing of Si<sub>3</sub>N<sub>4</sub> with Cr<sub>2</sub>O<sub>3</sub>,” *Philos. Mag. A*, vol. 74, no. 4, pp. 1003–1017, Oct. 1996, doi: 10.1080/01418619608242173.
- [11] A. Misra, P. M. Pandey, and U. S. Dixit, “Modeling of material removal in ultrasonic assisted magnetic abrasive finishing process,” *Int. J. Mech. Sci.*, vol. 131–132, pp. 853–867, Oct. 2017, doi: 10.1016/j.ijmecsci.2017.07.023.
- [12] S. A. Sirwal and A. K. Singh, “Analysis of the surface roughness for novel magnetorheological finishing of a typical blind hole workpiece,” *Proc. Inst. Mech. Eng. Part C J. Mech. Eng. Sci.*, vol. 233, no. 5, pp. 1541–1561, Mar. 2019, doi: 10.1177/0954406218776036.
- [13] V. K. Jain, *Advanced machining processes*. New Delhi: Allied Publishers, 2013.
- [14] S. Yang and W. Li, *Surface Finishing Theory and New Technology*. Berlin, Heidelberg: Springer Berlin Heidelberg, 2018.
- [15] D. K. Singh, V. K. Jain, V. Raghuram, and R. Komanduri, “Analysis of surface texture generated by a flexible magnetic abrasive brush,” *Wear*, vol. 259, no. 7–12, pp. 1254–1261, Jul. 2005, doi: 10.1016/j.wear.2005.02.030.
- [16] H. Yamaguchi, A. K. Srivastava, M. Tan, and F. Hashimoto, “Magnetic Abrasive Finishing of cutting tools for high-speed machining of titanium alloys,” *CIRP J. Manuf. Sci. Technol.*, vol. 7, no. 4, pp. 299–304, 2014, doi: 10.1016/j.cirpj.2014.08.002.
- [17] S. K. Amnieh, “Study on magnetic abrasive finishing of spiral grooves inside of aluminum cylinders,” *Int J Adv Manuf Technol*, p. 10, 2017.
- [18] J. Guo, H. Wang, M. Goh, and K. Liu, “Investigation on Surface Integrity of Rapidly Solidified Aluminum RSA 905 by Magnetic Field-Assisted Finishing,” *Micromachines*, vol. 9, no. 4, p. 146, Mar. 2018, doi: 10.3390/mi9040146.
- [19] Y. Gao, Y. Zhao, G. Zhang, G. Zhang, and F. Yin, “Polishing of paramagnetic materials using atomized magnetic abrasive powder,” *Mater. Manuf. Process.*, vol. 34, no. 6, pp. 604–611, Apr. 2019, doi: 10.1080/10426914.2018.1532087.
- [20] S. Ahmad, S. Gangwar, P. C. Yadav, and D. K. Singh, “Optimization of process parameters affecting surface roughness in magnetic abrasive finishing process,” *Mater. Manuf. Process.*, vol. 32, no. 15, pp. 1723–1729, Nov. 2017, doi: 10.1080/10426914.2017.1279307.
- [21] C.-T. Lin, L.-D. Yang, and H.-M. Chow, “Study of magnetic abrasive finishing in free-form surface operations using the Taguchi method,” *Int. J. Adv. Manuf. Technol.*, vol. 34, no. 1–2, pp. 122–130, Jul. 2007, doi: 10.1007/s00170-006-0573-8.
- [22] T. C. Kanish, P. Kuppan, S. Narayanan, and S. D. Ashok, “A Fuzzy Logic based Model to Predict the Improvement in Surface Roughness in Magnetic Field Assisted Abrasive Finishing,” *Procedia Eng.*, vol. 97, pp. 1948–1956, 2014, doi: 10.1016/j.proeng.2014.12.349.
- [23] R. K. Singh, S. Gangwar, D. K. Singh, and V. K. Pathak, “A novel hybridization of artificial neural network and moth-flame optimization (ANN–MFO) for multi-objective optimization in magnetic abrasive finishing of aluminium 6060,” *J. Braz. Soc. Mech. Sci. Eng.*, vol. 41, no. 6, p. 270, Jun. 2019, doi: 10.1007/s40430-019-1778-8.
- [24] P. Kala and P. M. Pandey, “Experimental Study on Finishing Forces in Double Disk Magnetic Abrasive Finishing Process While Finishing Paramagnetic Workpiece,” *Procedia Mater. Sci.*, vol. 5, pp. 1677–1684, 2014, doi: 10.1016/j.mspro.2014.07.356.
- [25] K. B. Judal, V. Yadava, and D. Pathak, “Experimental Investigation of Vibration Assisted Cylindrical–Magnetic Abrasive Finishing of Aluminum Workpiece,” *Mater. Manuf. Process.*, vol. 28, no. 11, pp. 1196–1202, Nov. 2013, doi: 10.1080/10426914.2013.811725.
- [26] Y.-H. Lee, K.-L. Wu, J.-H. Jhou, Y.-H. Tsai, and B.-H. Yan, “Two-dimensional vibration-assisted magnetic abrasive finishing of stainless steel SUS304,” *Int. J. Adv. Manuf. Technol.*, vol. 69, no. 9–12, pp. 2723–2733, Dec. 2013, doi: 10.1007/s00170-013-5242-0.
- [27] A. A. Moosa, “Utilizing a Magnetic Abrasive Finishing Technique (MAF) Via Adaptive Neuro Fuzzy (ANFIS),” *Am. J. Mater. Eng. Technol.*, p. 5.
- [28] P. Kala, S. Kumar, and P. M. Pandey, “Polishing of Copper Alloy Using Double Disk Ultrasonic Assisted Magnetic Abrasive Polishing,” *Mater. Manuf. Process.*, vol. 28, no. 2, pp. 200–206, Feb. 2013, doi: 10.1080/10426914.2012.746704.
- [29] A. C. Wang, L. Tsai, C. H. Liu, K. Z. Liang, and S. J. Lee, “Elucidating the Optimal Parameters in Magnetic Finishing with Gel Abrasive,” *Mater. Manuf. Process.*, vol. 26, no. 5, pp. 786–791, May 2011, doi: 10.1080/10426914.2010.505620.
- [30] N. Sihag, P. Kala, and P. M. Pandey, “Analysis of Surface Finish Improvement during Ultrasonic Assisted Magnetic Abrasive Finishing on Chemically treated Tungsten Substrate,” *Procedia Manuf.*, vol. 10, pp. 136–146, 2017, doi: 10.1016/j.promfg.2017.07.040.
- [31] E. Deniz, O. Aydogmus, and Z. Aydogmus, “Implementation of ANN-based Selective Harmonic Elimination PWM using Hybrid Genetic Algorithm-based optimization,” *Measurement*, vol. 85, pp. 32–42, May 2016, doi: 10.1016/j.measurement.2016.02.012.
- [32] H. Oktem, T. Erzurumlu, and F. Erzincanli, “Prediction of minimum surface roughness in end milling mold parts using neural network and genetic algorithm,” *Mater. Des.*, vol. 27, no. 9, pp. 735–744, Jan. 2006, doi: 10.1016/j.matdes.2005.01.010.
- [33] B. Stojanović, A. Vencl, I. Bobić, S. Miladinović, and J. Škerlić, “Experimental optimisation of the tribological behaviour of Al/SiC/Gr hybrid composites based on Taguchi’s method and artificial neural network,” *J. Braz. Soc. Mech. Sci. Eng.*, vol. 40, no. 6, p. 311, Jun. 2018, doi: 10.1007/s40430-018-1237-y.
- [34] G. Candan and H. R. Yazgan, “Genetic algorithm parameter optimisation using Taguchi method for a flexible manufacturing system scheduling problem,” *Int. J. Prod. Res.*, vol. 53, no. 3, pp. 897–915, Feb. 2015, doi: 10.1080/00207543.2014.939244.
- [35] S. Datta, C. Garai, and C. Das, “EFFICIENT GENETIC ALGORITHM ON LINEAR PROGRAMMING PROBLEM FOR FITTEST CHROMOSOMES,” p. 8, 2010.
- [36] K. Hanada, H. Yamaguchi, and H. Zhou, “New spherical magnetic abrasives with carried diamond particles for internal

- finishing of capillary tubes,” *Diam. Relat. Mater.*, vol. 17, no. 7–10, pp. 1434–1437, Jul. 2008, doi: 10.1016/j.diamond.2008.01.100.
- [37] H. Kumar, S. Singh, and A. Srivastava, “Parametric Investigations into Internal Surface Modification of Brass Tubes with Alternating Magnetic Field,” *Procedia Manuf.*, vol. 5, pp. 1234–1248, 2016, doi: 10.1016/j.promfg.2016.08.097.
- [38] D. K. Singh, V. K. Jain, and V. Raghuram, “Experimental investigations into forces acting during a magnetic abrasive finishing process,” *Int. J. Adv. Manuf. Technol.*, vol. 30, no. 7–8, pp. 652–662, Oct. 2006, doi: 10.1007/s00170-005-0118-6.
- [39] T. Mori, K. Hirota, and Y. Kawashima, “Clarification of magnetic abrasive finishing mechanism,” *J. Mater. Process. Technol.*, vol. 143–144, pp. 682–686, Dec. 2003, doi: 10.1016/S0924-0136(03)00410-2.
- [40] G. C. Verma, P. Kala, and P. M. Pandey, “Experimental investigations into internal magnetic abrasive finishing of pipes,” *Int. J. Adv. Manuf. Technol.*, vol. 88, no. 5–8, pp. 1657–1668, Feb. 2017, doi: 10.1007/s00170-016-8881-0.
- [41] H. J. C. de Souza et al., “Robust Design and Taguchi Method Application,” in *Design of Experiments - Applications*, M. Borges Silva, Ed. InTech, 2013.
- [42] R. K. Roy, *A primer on the Taguchi method*, 2nd ed. Dearborn, MI: Society of Manufacturing Engineers, 2010.
- [43] C.-X. Ma, K.-T. Fang, and E. Liski, “A new approach in constructing orthogonal and nearly orthogonal arrays,” *Metrika*, vol. 50, no. 3, pp. 255–268, Apr. 2000, doi: 10.1007/s001840050049.
- [44] R. Mead, “The Non-Orthogonal Design of Experiments,” *J. R. Stat. Soc. Ser. A Stat. Soc.*, vol. 153, no. 2, pp. 151–201, 1990.
- [45] C. M. Judd, G. H. McClelland, and C. S. Ryan, *Data analysis: a model comparison approach to regression, ANOVA, and beyond*, Third Edition. New York: Routledge, Taylor & Francis Group, 2017.
- [46] K. Wang, H. L. Gelgele, Y. Wang, Q. Yuan, and M. Fang, “A hybrid intelligent method for modelling the EDM process,” *Int. J. Mach. Tools Manuf.*, vol. 43, no. 10, pp. 995–999, Aug. 2003, doi: 10.1016/S0890-6955(03)00102-0.
- [47] V. C. Shukla, P. M. Pandey, U. S. Dixit, A. Roy, and V. Silberschmidt, “Modeling of normal force and finishing torque considering shearing and ploughing effects in ultrasonic assisted magnetic abrasive finishing process with sintered magnetic abrasive powder,” *Wear*, vol. 390–391, pp. 11–22, Nov. 2017, doi: 10.1016/j.wear.2017.06.017.
- [48] V. K. Jain, P. Kumar, P. K. Behera, and S. C. Jayswal, “Effect of working gap and circumferential speed on the performance of magnetic abrasive finishing process,” *Wear*, vol. 250, no. 1–12, pp. 384–390, Oct. 2001, doi: 10.1016/S0043-1648(01)00642-1.
- [49] K. Wang, G. L. Kovacs, M. Wozny, and M. Fang, Eds., *Knowledge Enterprise: Intelligent Strategies in Product Design, Manufacturing, and Management: Proceedings of PROLAMAT 2006, IFIP TC5 International Conference, June 15–17, 2006, Shanghai, China*, vol. 207. Boston, MA: Springer US, 2006.
- [50] A. Ghosh and S. Tsutsui, *Advances in Evolutionary Computing Theory and Applications*. Berlin: Springer Berlin, 2013.